WINDING NUMBERS AND MONODROMY OF VECTOR BUNDLES OVER A CIRCULAR BUFFER

Georg Essl

Department of Mathematical Sciences
University of Wisconsin - Milwaukee
Milwaukee, USA
essl@uwm.edu

ABSTRACT

The Möbius strip is perhaps the most recognizable topological object of general knowledge. It can be described mathematically in various ways including the formalism of line bundles. In this paper we discuss the bundle idea in the context of digital processing over a circular buffer and show how the idea leads to a more general notion known as monodromy, which describes the effect of the space on traversing a circle once. In this formulation, the monodromy of the Möbius strip is an orientation inversion characterized by a change in sign. This in turns leads to the concept of the winding number, which describes how many windings it takes to return to the original state. We discuss variable monodromy and illustrate that the winding number is robust under this variation. This will allow us to interpret previous disparate results in audio signal processing from Möbius waveguides to chaotic oscillators in delay loops in one unified framework. We close by showing how extending from line to vector bundles opens up the notion of braids to describe monodromy.

1. INTRODUCTION

The Möbius strip is perhaps the best known example from topology that transcends training and expertise. The non-orientability property, and its consequences, along with the simplicity of construction, make it a continued object of intrigue [1]. However, the Möbius strip behavior can also appear unexpectedly. Using a double cover argument, it was shown that mixed boundary conditions of 1-D wave equations behave like Möbius strips [2], which in turn explain effects such as halving of the fundamental frequency compared to boundary conditions that are not mixed. Examples of musical instruments with such properties are capped organ pipes, which are half the pitch of their uncapped counterparts, and reed wind instruments like the clarinet, which do not have to be as wound up as brass instruments for the same register range. Explicit construction of Möbius strip-like behavior in the modeling of a physical string goes back to Trautmann [3]. One aim of the current paper is to explain both of these approaches from the perspective of line bundles. This in turn allows us to connect this work to the work in matrix theory involving skew-circular shifts and skew-circulant matrices. This leads us to formulate an elementary form of a *Möbius circular buffer*.

Although various approaches to modeling the Möbius strip are well-known in the mathematical literature, they rarely make an appearance in digital signal processing, and if they historically did, the Möbius property was often only recognized after the fact. For example, the Johnson counter [4], was developed to minimize the number of physical gates in digital ring counter design. It uses one inversion between flip-flop stages to double the number of states that can be captured in a circular (ring) shift configuration. This has since been realized to be essentially a Möbius strip and hence this counter is sometimes called twisted or Möbius counter [5].

In this paper we want to discuss the Möbius strip in the context of interpreting the digital signal processing on circular buffers in terms of line bundles over a discrete circular space. Extending the line bundle from real to complex data leads to the notion of a circle bundle as well as to the notion of a 2-dimensional real vector bundle. We develop intuitive yet central concepts in a setting familiar to audio signal processors, such as the notion *monodromy* [6], the change of behavior as one goes around a loop once, and the related concept of the *winding number* [7], which in our context counts how often we have to wind around a loop to return to an identical state. This concept is also known as *periodic orbit* in the nonlinear dynamics literature [8]. By accumulating the effects of monodromy, we arrive at the winding number. Monodromy describes local behavior, while the winding number describes the global consequence thereof. We anchor our discussion on the familiar notion of a circular buffer and define monodromy on this structure.

Specifically, we will describe the real and complex *line bundle*, though the complex case could also be called the *circle bundle*, and describe how the notion can be extended to finite-dimensional *vector bundles*. Following the lead of work on chaotic oscillators inside circular buffers by Berdahl-Sheffield-Pfalz-Marasco [9] we discuss how nonlinear local discrete one-step iterations fit into analysis of periodic orbits on circle bundles, leading to concrete examples of vector bundles and illustrate the robustness of the winding number to characterize fundamental frequencies. We use the visual notion of *braiding* to suggest intuitive ways to think about windings from interconnected circular buffers of a finite-dimensional vector bundle, and giving us a way to interpret the double cover pictures from Essl [2].

2. RELATED WORK

In recent years, topology has found increasing applications in audio signal processing and synthesis [11, 12]. These ideas live in a broader development of fields of topological data analysis, topological signal processing [13], and the emergence of applied and computational topology as a branch of topology, mathemat-

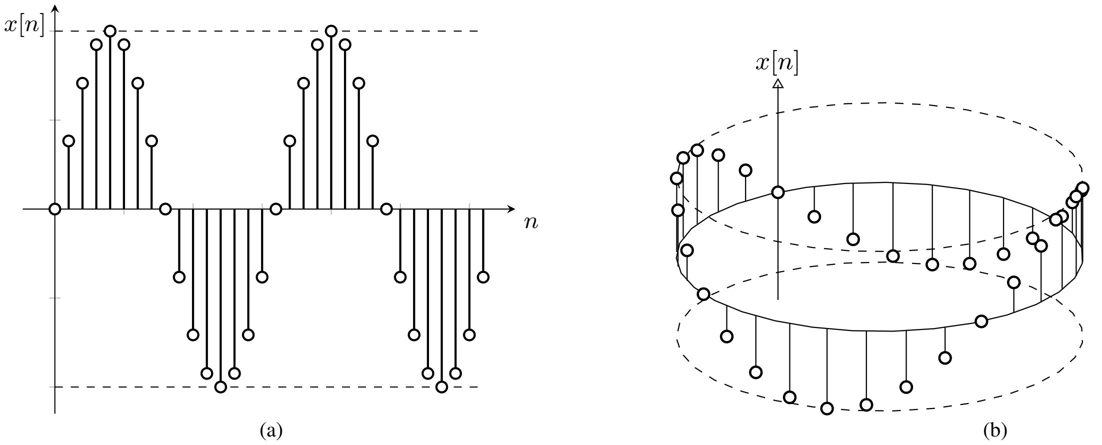

Figure 1: A finite discrete sequence of 32 samples $x[n]$ of a sampled sine of period 16. (a) $\mathbb{I}_{[N]}$: sample sequence domain with boundaries at 0 and $N-1$. (b) $\mathbb{I}_N$: sample sequence domain without boundaries on a discrete circular domain of period N (from [10])

ics, and theoretical computer science which advances topological techniques with applied relevance [14].

Within the context of applied and computational topology, applied uses of vector bundles have been investigated [15, 16] outside of audio signal processing. Within signal processing, a related proposal is the use of graph fibers [17]. Applications of real and complex vector bundles have also found numerous applications in computer graphics [18].

Trautmann [3] gave the first explicit construction of a synthesis method on a Möbius strip. He constructed a waveguide model of the wave equation as interpreted living on the strip. The realization that mixed Dirichlet-Neumann boundary conditions of the 1-D wave equation constitute a Möbius strip was given in Essl [2] using a topological double cover argument over loops.

The discussion in this paper uses fiber bundles as fundamental building blocks [19]. These are closely related to sheaves [20], which play an important role in many topological signal processing approaches [13]. An intuition for the how these concept relate in the context or our discussion is the following: Finite dimensional vector bundles are related to sheaf-based models using finite vector spaces whose dimension stays constant.

Skew-circular shifts, and skew-circulants, though without the Möbius interpretation, are classical topics in the theory of matrices [21, 22, 23]. The skew-circular shift was explored in the context of digital signal processing in connection with number-theoretic methods in signal processing [24] but without a geometric or topological explanation and in the context of more recent efforts to develop a theory of algebraic signal processing [25]. The theory of vector bundles is well-established within algebraic topology [26].

Vector bundles, including the use of line bundles to describe the Möbius strip, were investigated in the context of mathematical control theory [27]. Monodromy, although usually without the use of vector bundles, appeared in the study of periodic differential equations and dynamical systems [28] and was used as part of generative audio systems [29].

Despite all this, there is a lack of exposition that brings these ideas together. The occurrence of Möbius strips and the role of twists do not appear to be common knowledge in audio signal processing and synthesis, and the use of skew-circular shifts [30] and monodromy [31, 32] is rare. Hence, providing an accessible exposition of these sets of ideas is an additional goal of this paper.

3. FROM INTUITION TO FORMALISM: LINE BUNDLES

The distance from a more general abstract mathematical notion to a familiar setting in digital signal processing is at times much shorter than one might fear. When it comes to line bundles, an argument can be made that we are familiar with the notion at least implicitly. We often depict digital signals as data samples over a discrete time line, viewing the relationship between time and sample as a Cartesian product in the Euclidean plane to show graphs. This depiction is found in Figure 1(a). Although perhaps less frequently, yet still rather comfortable are the circular arrangements of samples to depict a signal in a circular buffer , as is seen in Figure 1(b) (Figures from [10].

The Euclidean plane in which we depict this figure does a lot of work for us in this context. If we compare one sample to the next, we assume that they all are comparable with respect to their scale with regard to the axis, which in turn lives in this plane. The idea of *fiber bundles* is to think of this plane as being decomposed into the individual samples, and that we explicitly describe how the space on which one sample exists corresponds to the space of the next sample. Imagine that Figure 1 was cut into vertical strips that each contained only one sample. We want to specify how these individual strips should be assembled. Notice that it is best to think of these strips as independent from the actual sample data. They are lines along the vertical axis that allow for all possible values of the sample data. You could have a sample with a different amplitude on the line. So in this sense, we are concerned with the underlying space on which the sample lives. This is directly analogous to having storage for a sample that we shift and manipulate. The storage allows for all possible samples of a type, but connected storage might specify how they transfer samples between each other. In the bundle perspective, we call the storage a *fiber*.

An important aspect of this decomposition of space per sample is that we use only the discrete (possibly circular) order of the underlying discrete time line. It is flexible how these samples actually correspond to some reference time. In this sense, we have liberated ourselves from a hard-embedded version of signals, to a more topological perspective of the space the signal lives on. This emphasizes the notion that the transfer of data between positions specifies everything of interest, not how data lives in some sub-

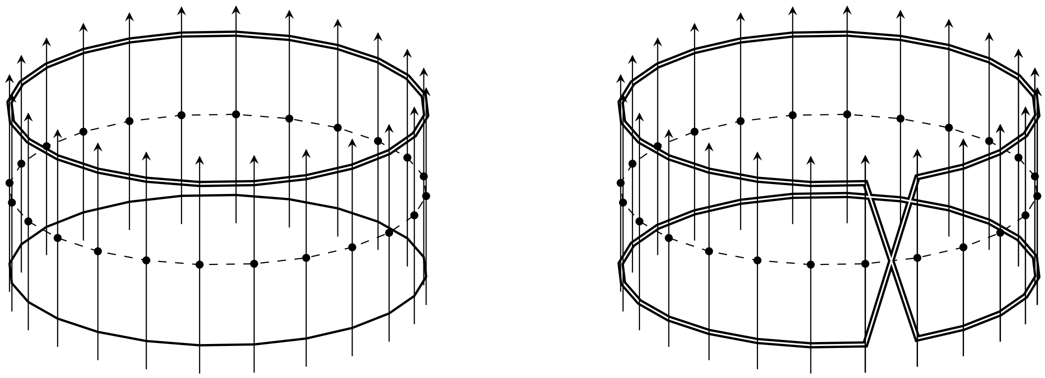

(a) (b)

Figure 2: Line bundles of a circular buffer of length 16. (a) Trivial Line Bundle as corresponding to the classic circular buffer. (b) Möbius Strip via a Line Bundle with a twisted identification, corresponding to a circular buffer with one sign inversion in the loop.

strate space. Hence, this is also a more intrinsic view of data, and is applicable to numerous embeddings.

Perhaps we want to specify only the orientation and nothing else. If we keep the original orientation between two neighboring fibers, this is equivalent to multiplying the underlying data by 1. If we want to flip the orientation between neighboring fibers, we multiply the underlying data by -1. But we want to view this map as a linear map between fibers.

Therefore, consider the data in the fiber to be a one-dimensional vector space $\mathbb{R}$, and the map between neighboring fibers is indeed a linear map $t : \mathbb{R} \to \mathbb{R}$. The map t is called *transition map* in the literature on fiber bundles [26]. In general, a vector bundle can be completely described by transition maps alone [19].

For our discussion, we will further require that it is a unitary map. This means that the data between fibers is not rescaled. This can be generalized to isomorphic maps, but we will stick to this reduced setting because all the effects we care about can already be seen in this case.

A *fiber bundle* E collects this information together. It consists of the base space B and the fibers F. Each fiber is attached to a point of the base space, so we always have a way to get from a fiber in the bundle E to its base point B via a projection $\pi : E \to B$. Locally, this looks like the Cartesian product $F \times B$ that we would traditionally use globally to define the graph of Figure 1(a). We will only consider fibers that are finite-dimensional vector spaces, which in turn are called *vector bundles*, and they can be real or complex.

In this paper, the base space is a discrete circle, which one can think of the usual circle subdivided into n segments and the original distances disregarded. Visually, it looks like n discrete points in with a circular order. Fibers are always either real or complex finite-dimensional vector spaces, and transition maps are always invertible linear maps between fibers.

Bundles are usually considered over more general topological spaces than just finite discrete ones, where (co)limits are important to keep track of data as one zooms in and out. However, given that we deal with finite discrete spaces, this particular feature does not play any role for us, leading to a much simpler picture. In particular, it allows us to consider only neighboring transition maps for our discussion rather than the picture of all possible transition maps of growing and shrinking neighborhoods and their overlap.

4. CLASSIC AND MÖBIUS CIRCULAR BUFFERS

The customary circular buffer, which we will give the attribution *classic*, is what is called a *trivial line bundle*, which is formalized as saying that all transition maps are identity maps. For a line bundle, this means that the transition map, a scalar multiplication, is 1 everywhere. This is depicted in Figure 2(a) the double line indicates the unit position. If we introduce a -1 transition between two neighboring fibers locally, we end up with Figure 2(b). For the signal, this means that we flip the sign of the signal at one transition in the circular loop. The location of the sign change is clearly indicated by the crossing lines. Notice that, essentially by definition, this line bundle is not trivial, but we also immediately see what that means. Due to the crossing of what used to be a single double line on each fiber, we now have two double lines on each fiber. This is one of the ways one can characterize the Möbius strip. As one follows along one rim of the strip, one will actually traverse both rims before returning to where one started. During this process, one will traverse both signs (or "orientations"), which means that unlike in the case of the trivial line bundle, we cannot choose the orientation. This is the topological property for which the Möbius strip is famous. The pattern of the double line in Figure 2(b) is the double cover picture given in [2], which is, however, derived from mixed boundary conditions of a digital waveguide leading one reflection flipping the sign as depicted in Figure 3(right). In Trautmann's work two copies of this structure are present because the vibration is modeled to occur on a Möbius strip and both left and right traveling waves of the d'Alembert solution are modeled, and each has to follow the underlying topology of the strip as seen in Figure 4(b). The *Möbius circular buffer* of Figure 4(a) hence appears twice. As we will see next this structure described as a special case of r-circular shift matrices.

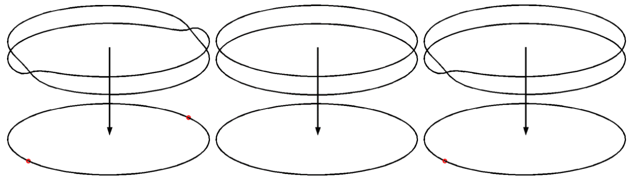

Figure 3: Double covers of a 1-D waveguide for (left) two signed (middle) no signed and (right) one signed reflections [2].

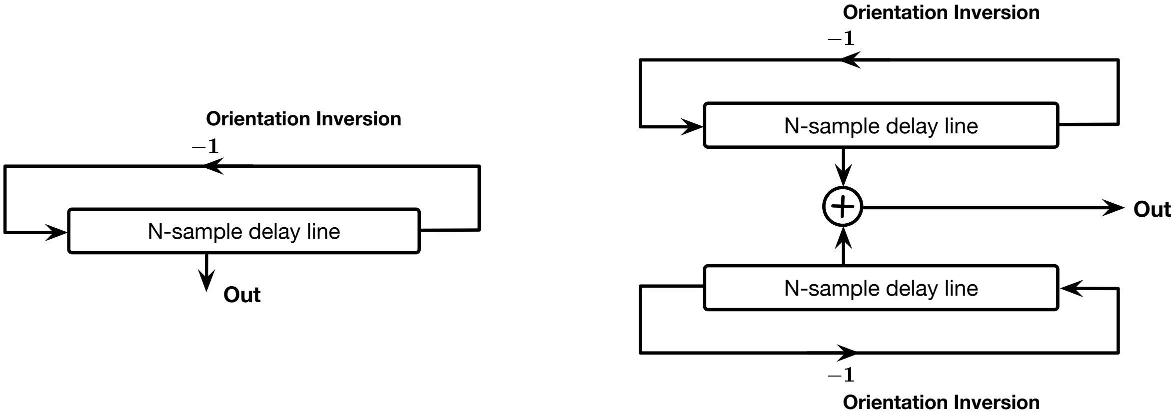

(a) Möbius circular buffer

(b) Trautmann's commuted waveguide on a Möbius strip.

Figure 4: Versions of Waveguide models of the Möbius circular buffer. (a) The elementary Möbius circular buffer interpreted as a commuted waveguide of mixed boundary conditions. (b) The commuted version of the twisted waveguide modeling a string on a Mobius strip after Trautmann [3].

5. MATRIX REPRESENTATION OF r-CIRCULAR SHIFTS

A circular shift can be represented as a matrix operator. All our matrix operators are finite square matrix of some fixed size n corresponding to the length of the circular buffer. An element is copied by unit multiplication from one position to a neighboring position, and the old content is erased by a multiplication by 0. Hence, the matrix captures the directional transition from one discrete fiber to its neighbor, and can equivalently be constructed from adjacency relationships of the underlying domain [25]. If our matrix contains only entries of 1, we recover the classic circular shift C. The Möbius (twisted, or skew) circular shift M inverts the sign on one transition in the cycle. Both of these cases can be encapsulated in an r-circular shift [21]. Up to convention of shift direction we chose the following form of the circular shift:

$$A = \begin{bmatrix} 0 & 1 & 0 & \cdots & 0 \\ 0 & 0 & 1 & \cdots & 0 \\ \vdots & \vdots & \ddots & \ddots & \vdots \\ 0 & 0 & \cdots & 0 & 1 \\ r & 0 & \cdots & 0 & 0 \end{bmatrix} \tag{1}$$

where choosing $r = 1$ recovers $C := A(r = 1)$ and $r = -1$ recovers $M := A(r = -1)$. Clearly both of these cases lead to real unitary matrices, and we have an immediate generalization to complex unitary matrices if $r \in \mathbb{C}, r = a + ib, a, b \in \mathbb{R}$, $|r| = \sqrt{a^2 + b^2} = 1$.

Assume that we have a discrete circle base space of n samples, then we can represent the signal on each fiber as a vector at some discrete time index t as $v_t[0, \ldots, n-1]^T$ of $n \in \mathbb{N}$ values in $\mathbb{R}$ and the effect of a discrete time step is the operation: $v_{t+1} = Av_t$.

None of our discussion differs based on the shift direction, and hence we will assume one first direction for the shifts without loss of generality. However, construction in the opposite direction of (1) is straightforward as the opposite direction clearly is the inverse, which, given that these matrices are clearly orthogonal, is the adjoint. Hence, the opposite shift is $A^{-1} = A^T$ if $r \in \mathbb{R}$. Given that r preserves the (complex) unitarity of A the inverse in this case is the complex conjugate transpose $A^{-1} = A^*$. The underlying geometric intuition comes from the multiplication by a unitary complex number r acting as a rotation in the complex plane. The complex conjugate yields the same rotation in the opposite direction.

6. MONODROMY AND WINDING NUMBER

The monodromy describes the effect that is observed as one traverses a loop once. We can formalize this by asking what happens when we apply the shift operator to a circular buffer n times, where n is the length of the buffer. This is equivalent to completing one loop or cycle. Hence, we have $\mu = A^n$. For the classic circular buffer C we observe that the monodromy $\mu_C = C^n = I$ is the identity. This means that when we shift a circular buffer n times we get back to where we started (which is the same as never having shifted at all). The monodromy in this case is not particularly interesting.

However, observe that for the monodromy of the Möbius circular buffer $\mu_M = M^n = -I$ we get the negative identity matrix. So the Möbius circular buffer inverts the sign of the signal. If we take the more general case of the r-circular buffer A we have $\mu_A = rI$.

If we go around the Möbius circular buffer twice, we observe that we recover the identity:

$$\mu_M^2 = M^{2n} = I \tag{2}$$

Traversing around a Möbius strip means going through both orientations in succession to return to the identity. This is an alternative way to think about its non-orientability.

This setup suggests the question: For a more general r-circular buffer, can we find the identity by repeatedly applying its monodromy μ_A? Is there a finite number $w \in \mathbb{N}$ for which $\mu_A^k \neq I \forall k < w \in \mathbb{N}$ and $\mu_A^w = I$? If the answer is yes, we call w the *winding number*. The winding number counts how many times we have to complete n-shifts around the loop to return to the starting configuration. As we already saw from equation (2) that the winding number for the Möbius circular buffer is 2, while the winding number of the classic circular buffer C is 1. The winding number gives us an immediate comparison between the number of completed loops needed to return to the identity between different monodromies. For example, the ratio between the classic and the Möbius circular buffer is $1:2$.

If we only consider unitary real r-circular buffers, there are only two possible unitary values, -1 and 1 hence we have already covered this case completely. This observation holds for shift matrices with arbitrary numbers of -1 and 1 entries in the following way: If the number of -1 entries is odd, the monodromy is $-I$, otherwise it is I. The monodromy does not capture finer detail than the parity of sign changes per completed loop.

If we consider unitary complex r-circular buffers, any multiplication by a unitary complex number r constitutes a pure rotation in the complex plane. Rotations are finitely periodic if and only if they can be expressed as rational numbers relative to the circumference. Hence, monodromy can be expressed for $r = e^{i2\pi c/d}$ where $c, d \in \mathbb{N}^+$ with $c \leq d$. To arrive at a closed circle using rational increments we have $r^w = e^{i2\pi c/d \cdot w} = e^{i2\pi} = 1$ hence naively we will have a closed winding after d iterations. However, we are interested in the first closed loop, which can occur earlier if c and d share a common divisor. Hence, we have $w = d/\gcd(c, d)$. For example, if we progress by $2/3$ of a circle, we have $w = 3$.

6.1. Topological interpretation of invertible line maps

The unitary complex numbers form a circle topologically, hence we can think of the unitary complex line bundle also as a circle bundle. In fact, even the unitary real numbers can be thought of as a 0-dimensional circle, which consists of two disconnected points [26]. This is a more topological interpretation of the above observations. The real case offers two distinct but discrete possibilities, while the complex case offers a continuous choice in principle but, having a rational subset from which we draw constructions with finite winding numbers.

Setting aside stability considerations, this argument extends to non-unitary cases as follows [33]: The class of general linear invertible maps $\mathbb{R}^* := GL(1, \mathbb{R}) = \mathbb{R} \setminus \{0\}$ is the real line without the 0 element, hence is disconnected at this point, hence still separating orientation. $\mathbb{R}^*$ is homotopic to two separate points. This indicates that there is an essential topological separation of all invertible linear maps on $\mathbb{R}$. On the other hand $\mathbb{C}^* := GL(1, \mathbb{C}) = \mathbb{C} \setminus \{0\}$ are all non-zero complex numbers under multiplication, of which the unitary complex numbers are a subset. $\mathbb{C}^*$ is homotopic to the circle.

7. SPECTRAL BEHAVIOR

Circular shifts have a fundamental relationship to discrete Fourier transforms. Circulant matrices is the matrices of all possible circular m-shifts, $m = 1, \ldots, n-1$ as off diagonals. The discrete Fourier transform diagonalizes circulant matrices. In diagonal form, the spectrum can be read off from the diagonal. In other words, the DFT moves from a shift perspective (circular convolution) to a spectral perspective (eigenvalues in the diagonal) and vise versa. A completely parallel construction for r-circular shifts and r-circulant matrices and their diagonalization, which includes the case that $r = -1$, which is known as skew-circulant [21, 24].

The monodromy of the circular shift already suggests how we get eigenvalues. Given that eigenvalues are the scalars of the diagonalized matrix, which is indeed achieved by n cyclic shifts. It follows from $\mu_A = rI$ that the eigenvalues must be:

$$\lambda^n = r \tag{3}$$

Since $|r| = 1$, all solutions of $\lambda^n = r$ lie on the unit circle. We will enumerate the n roots of unity with the index $k = 0, 1, \ldots, n-1$. Therefore, the spectrum is shifted by the set of the n distinct nth roots of r.

$$\lambda(A)_k = r^{1/n}\omega_n^k \tag{4}$$

where $\omega_n = e^{2\pi i/n}$ is the familiar nth root of unity and $r^{1/n}$ denotes any fixed choice of an nth root of r. This provides the general solution for any r, including irrational ones. We call $r^{1/n}$ the *monodromy modulation* of the spectrum of the classic circular buffer.

Classic circular shift: If $r = 1$ then this is just the standard spectrum of a circular shift.

$$\lambda^n = 1 = e^{i2\pi} \tag{5}$$

The eigenvalues are:

$$\lambda(C)_k = \omega_n^k = e^{i(2\pi k)/n} \tag{6}$$

Möbius circular shift: If $r = -1$ the monodromy requires that:

$$\lambda^n = -1 = e^{i\pi} \tag{7}$$

Observe that the Euler identity describes precisely the case of the Möbius circular buffer spectral shift. The eigenvalues are:

$$\begin{aligned}\lambda(M)_k = e^{i\pi/n}\omega_n^k &= e^{i(\pi+2\pi k)/n} \\ &= e^{i2\pi(2k+1)/2n}\end{aligned} \tag{8}$$

Subharmonic circular shift: If $r = e^{i2\pi\theta}$ with a complex rotation that is a uniform subdivision of the full rotation such that $\theta^m = 1$:

$$\theta = e^{i(2\pi)/m} \tag{9}$$

$$\lambda^n = \theta = e^{i(2\pi)/m} \tag{10}$$

The eigenvalues are:

$$\begin{aligned}\lambda(A)_k = \theta^{1/n}\omega_n^k &= e^{i2\pi(1/m+k)/n} \\ &= e^{i2\pi(mk+1)/mn}\end{aligned} \tag{11}$$

7.1. Fundamental frequencies

We will call the lowest possible oscillatory frequency, the *fundamental frequency*. The fundamental frequency for the standard circular spectrum is found at $l = 1$, since $l = 0$ is the constant function, we have an angular frequency $2\pi/n$. All other cases are subject to monodromy modulation. Its effect of monodromy modulation in general is to lift the case $l = 0$ away from being constant. For the Möbius circular shift we find that the fundamental frequency occurs at $k = 0$ and is π/n. This confirms a number of properties of the Möbius strip. The absence of a constant function in the spectrum reflects the non-triviality of the line bundle. The halving of the fundamental frequency reflects the doubling of the winding number (usually called wavelength) due to the need to traverse the circle twice to close the loop. This is a well known property of musical instruments that are well approximated by mixed boundary conditions such as capped organ pipes and reed instruments [34, 2]. In general, a subharmonic monodromy modulation leads to a fundamental frequency at $l = 0$ of $2\pi/(mn)$, hence the larger m, which corresponds to a smaller subdivision of the circle, the lower the fundamental frequency.

7.2. Harmonics

Only the spectrum of the classic circular shift allows for a constant solution, which is excluded as the lowest oscillatory frequency. For this reason, it seems that the frequencies are shifted down with monodromy. However, technically, all frequencies are shifted up by monodromy as a consequence of the monodromy modulation of equation (4). This observation is crucial for really understanding the changes in harmonic components in the spectrum. This also explains the odd harmonics in the Möbius case, because the 0th eigenvalue becomes the lowest oscillatory frequency and all other frequencies are also shifted up. By adding a constant $1/2$ to the harmonic index starting with 0 we get $0 + \frac{1}{2} = \frac{1}{2}, 1 + \frac{1}{2} = \frac{3}{2}, \ldots, (n-1) + \frac{1}{2} = \frac{2n-1}{2}$. Given that division by 2 is a shared factor, when viewing harmonics as ratios, we arrive at an odd-harmonic spectrum. This is the observed spectrum of straight pipe wind instruments, where one end effectively acts as closed while the other is open, such as the clarinet and its precursor, the chalumeau, and capped organ pipes [34].

The same argument predicts that the harmonics starting with the "subharmonic" fundamental frequency of $r = e^{i(2\pi/m)}$ are $k + \frac{1}{m} = (mk+1)/m$. This leads to an increasingly sparse harmonic sequence the bigger m. For example, for $m = 7$ we see that the present harmonics are located at $1, 8, 15, 22...$ This is a consequence of the harmonics of the original circular buffer. The spacing between harmonics is not changed by the modulation introduced, but the lowest frequency decreases, leading to an apparent spreading of the harmonics, which, however, are effectively only shifted up somewhat from their original circular buffer harmonics positions. Paradoxically, the lower the subharmonic, the milder the shift of spectral frequencies from the original position, yet the more severe the apparent spread of harmonics.

8. VARIABLE MONODROMY AND NONLINEARITY

So far we have discussed examples that can be thought of as stepping around the complex circle in uniform steps. This leads to straightforward relationships between monodromy, winding number, and spectral properties. From a topological perspective, this is rather rigid. To make these ideas more flexible, consider the circumference of the complex circle in the complex line bundle and consider a trajectory of points on the circle to itself that form a finite periodic sequence of length w, also known as *periodic orbits* [8]. In other words, we fix a winding number, but we no longer require that the monodromy be fixed for each winding. An example of a 4-periodic orbit of this type is shown in Figure 6(a).

An individual sample will only be modified by the monodromy every full cycle, and specifically at one periodic time step. This means that for an individual sample we can define a relationship of monodromy and winding number as follows:

$$A_{t+0}, A_{t+n}, \ldots A_{t+(w(t)-1)n} = \prod_{j=0}^{w(t)-1} \mu_j(t) = I \qquad (12)$$

with $t = 0, \cdots, n-1$ corresponding to the position relative to the monodromy in the circular shift matrix. Notice that each sample has an independent monodromy, with the benefit that each can be studied independently. To study this general setting is beyond the scope of this paper. We will instead focus on the case of one sample under variable monodromy. Without loss of generality, assume

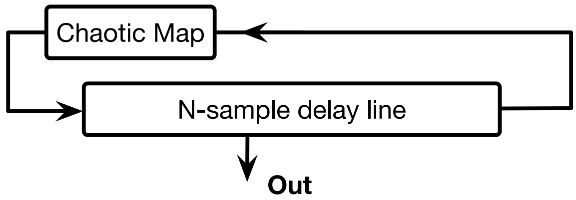

Figure 5: Chaotic iterations as variable monodromy in a circular buffer after Berdahl-Sheffield-Pfalz-Marasco [9].

that $t = 0$ we get:

$$A_0, A_n, \ldots A_{(w-1)n} = \prod_{j=0}^{w-1} \mu_j = I \qquad (13)$$

where μ_j is the variable monodromy per full circular shift. w is the winding number. Clearly, we observe that w defines the periodicity of the map, an observation that goes back to Poincaré, and its limit behavior can also be used to describe the behavior of trajectories that are not periodic orbits [8].

8.1. Chaotic Oscillator within a Circular Buffer

This setting gives a direct interpretation of an observation of chaotic oscillators within a circular buffer as proposed by Berdahl-Sheffield-Pfalz-Marasco [9] in order to improve controllability of chaotic oscillators. Their structure is depicted in Figure 5.

A one-dimensional chaotic map on the circle is simply the iterative relationship:

$$r_k = f(r_{k-1}) \qquad (14)$$

where $f : \mathbb{S}^1 \to \mathbb{S}^1$ is an arbitrary, usually highly non-linear, map. We observe that it gives a fixed numeric relationship between r_k and r_{k-1}, hence for our purpose f simply gives us the factor r for each shift. This iteration is modified [9] to use as the past value the value of the full circle delay. Hence, we have:

$$r_k = f(r_{k-n}) \qquad (15)$$

Discrete, deterministic, chaotic oscillatory maps contain a rich tapestry of phenomena. One of them is the ability to form finite periodic orbits for certain inputs [8].

While this discussion can be had for any stable non-linear iterative map (of which a number are discussed in [9]), we will pick the case of the sine circle map (also known as feedback frequency modulation) [35]. This map has the advantage of being topologically stable [35], which means that it is unconditionally stable due to being intrinsically defined on a circle topology.

The phase iteration for the sine circle map is:

$$x_k = x_{k-1} + \Omega + \frac{K}{2\pi} \sin(2\pi x_{k-1}) \mod 1 \qquad (16)$$

Each value of the iteration x_k acts as the monodromy μ_k.

Each discrete step is modeled corresponds to a complex linear map (a complex rotation). hence, we are modeling the nonlinear function that generates the map by linear transition maps for each step. However, this is not guaranteed to be globally linear as the map varies. Furthermore, the finite periodic orbits we are considering is a subset of all possible behavior of the nonlinear function

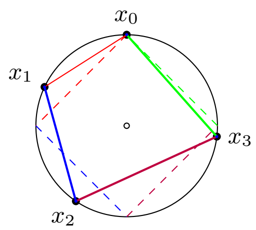

(a) Periodic orbit on the circle

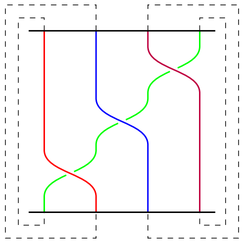

(b) Its braiding pattern

Figure 6: Invariance of the braiding pattern to orbit shape. Comparing uniform orbit from $r = i$ (dashed) to a non-uniform orbit generated from the sine circle map (solid) [parameters $K = 0.5$, $\Omega = 0.2595132507162096$, $x_0 = 0.25$]. (a) Positions in the unitary complex line (circle) bundle. (b) Braiding pattern of both monodromies is identical.

(16) under iteration. However, it allows us to discuss the periodic orbit case explicitly.

Berdahle *et al* [9] observed that "the tones will tend to be centered around f_S/L (or subharmonics of this if the state vector is multidimensional)" where L is the length of the circular buffer (our n). We arrive at a refinement of this observation. The frequency observed is the one of the periodic orbit's winding number, and even in the case of real iterators, we should expect the possibility to observe that Möbius case $r = -1$, hence the period doubling.

9. VECTOR BUNDLE MONODROMY VIA BRAIDS

Complex line bundles can also be viewed as a 2-dimensional real vector bundle. In principle, one can consider any finite dimensional real or complex vector bundle and associate with each dimension a circular buffer of shared length n, then monodromy behavior can be defined in a straightforward generalization, by moving monodromy from scalar multiplication to matrix multiplication. Although monodromy, can in full generality involve rather general matrices with broad restrictions (such as determinant having to be ± 1), we will restrict ourselves to a sketch of a particularly topological subset of all such matrices, namely those that lead to braids [36]. This in turn allows us to see identical patterns through difference in variable monodromy.

Braids shows the effect of monodromy on separate states within one or more loops. We have seen two ways we can get monodromy: (1) Having separate states such as a sign change of $\mathbb{R}^*$, or (2) by interconnecting bases in the vector space corresponding to multiple loops. Identity and sign inversion of $\mathbb{R}^*$ within one circular buffer are depicted as braid diagrams in Figure 7, but the same pattern also describes the cross-connection of two circular buffers (dashed line).

This picture gives us an immediate interpretation of the non-reflecting boundary condition double cover of [2] as depicted in Figure 3(middle), which is identical to the case shown in Figure 7(b), while Figure 7(a) gives a braid explanation of the Möbius behavior on the circular buffer as given as double cover in Figure 3(right). The case of two reflecting boundary conditions as double cover pictures (Figure 3(left)) discussed in [2] does not have a direct interpretation in our setting due to the presence of only one local monodromy. A straight-forward extension to allow that case would require a kind of "half-monodromy", to localize the second reflection.

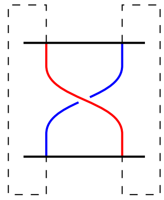

(a) $r = -1$

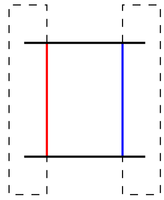

(b) $r = 1$

Figure 7: Identity and sign inversion as elementary braid moves. The dashed lines correspond to the connection of the braid through the circular buffer. While only one real circular buffer is needed, there it can contain a signal or a sign-inversion thereof.

However, these braid constructions can be composed to form more complicated braiding patterns. For example, if the monodromy r is in i the monodromy sequence is $i, -1, -i, 1$. In the language of the 2-dimensional real vector bundle, this becomes a matrix:

$$M = \begin{bmatrix} 0 & 1 \\ -1 & 0 \end{bmatrix} \tag{17}$$

One off-diagonal entry captures the real-imaginary axis exchange, while the sign captures the sign change induced by squaring i. So, while the complex numbers are only a 2-dimensional real vector space, due to the sign inversion of the squaring sign, we get a winding number of 4. The iterated multiplication by i contains a Möbius twist!

The flexibility of the winding number and braids is illustrated in Figure 6. It shows two examples that we discussed earlier: The case of fixed monodromy $r = i$ of a complex line bundle and an example of a 4-period orbit generated by the sine circle map. Their braid pattern (shown in Figure 6(b) is identical, as is their winding number. Braids help us abstract away the concrete monodromies in terms of angular intervals and instead encode which monodromy connectivity is shared between these cases.

10. CONCLUSIONS

In this paper, we described a discrete line bundle interpretation of the circular buffer with a local unitary twist in the loop. This allows us to give elementary interpretations of topological constructions by Trautmann [3] and Essl [2] in a unified framework. By considering unitary complex line bundles, which are equivalently circle bundles, we discussed more complicated periodic patterns, including a methodology for analyzing nonlinear discrete oscillators within the loop [9] via the notion of variable monodromy.

Monodromy and braids are also an active research topic in persistent homology [37]. Such braiding can also be interpreted as knots, which recently have found applications in musical interface design [38]. Specifically, the topic of higher dimensional vector bundles was only sketched here, and connections to multi-delay methods such as feedback delay networks [39] remain to be explored. Exploring vector bundles and, more generally, sheaves in all these directions is interesting future work.

11. ACKNOWLEDGMENTS

Many thanks to three anonymous reviewers for their insightful comments, which helped improve the final version of this paper.

12. REFERENCES

[1] K. Möbius, M. Plato, and A. Savitsky, *The Möbius Strip Topology: History, Science, and Applications in Nanotechnology, Materials, and the Arts*. Jenny Stanford Publishing, 2022.

[2] G. Essl, "Aspects of the topology of interactions on loop dynamics in one and two dimensions," in *International Symposium on Computer Music Modeling and Retrieval*. Springer, 2004, pp. 220–231.

[3] S. Trautmann, "A Physical String Model with a Twist," in *Proceedings of the International Computer Music Conference (ICMC)*, 1995.

[4] R. R. Johnson, "Electronic counter," US Patent 3,030,581, 1958.

[5] L. W. Cox, "A digital timing system for a biomedical data acquisition system," Ph.D. dissertation, Texas Tech, 1974.

[6] H. Żołądek, *The Monodromy Group*. Birkhäuser, 2025.

[7] J. Roe, *Winding Around – The Winding Number in Topology, Geometry, and Analysis*. American Mathematical Society, 2015.

[8] B. Hao and W. Zheng, *Applied symbolic dynamics and chaos*, ser. Peking University - World Scientific advance physics series vol. 4. World Scientific, 2018.

[9] E. Berdahl, E. Sheffield, A. Pfalz, and A. T. Marasco, "Widening the razor-thin edge of chaos into a musical highway: Connecting chaotic maps to digital waveguides." in *NIME*, 2018, pp. 390–393.

[10] R. Belton and G. Essl, "Discrete level set persistence for finite discrete functions," *Foundations of Data Science*, vol. 10, pp. 113–157, 2026.

[11] G. Essl, "Topology in Sound Synthesis and Digital Signal Processing–DAFx2022 Lecture Notes," *arXiv preprint arXiv:2211.05821*, 2022.

[12] ——, "Combinatorial Hodge Theory in Simplicial Signal Processing – DAFx2023 Lecture Notes," *arXiv preprint arXiv:2311.03469*, 2023.

[13] M. Robinson, *Topological Signal Processing*, ser. Mathematical Engineering. Springer, 2014.

[14] T. K. Dey and Y. Wang, *Computational Topology for Data Analysis*. Cambridge University Press, 2022.

[15] A. Singer and H.-t. Wu, "Orientability and diffusion maps," *Applied and computational harmonic analysis*, vol. 31, no. 1, pp. 44–58, 2011.

[16] L. Scoccola and J. A. Perea, "Approximate and discrete euclidean vector bundles," in *Forum of Mathematics, Sigma*, vol. 11. Cambridge University Press, 2023, p. e20.

[17] T. M. Roddenberry and S. Segarra, "Windowed fourier analysis for signal processing on graph bundles," in *International Conference on Acoustics, Speech and Signal Processing (ICASSP)*. IEEE, 2023, pp. 1–5.

[18] F. Knöppel and U. Pinkall, "Complex line bundles over simplicial complexes and their applications," in *Advances in discrete differential geometry*. Springer, 2016, pp. 197–239.

[19] A. S. Mishchenko, *Vector Bundles and Their Applications*. Springer, 1998.

[20] D. Berwick-Evans, A. N. Hirani, and M. D. Schubel, "Discrete vector bundles with connection," *arXiv preprint arXiv:2104.10277*, 2026.

[21] P. J. Davis, *Circulant matrices*. Wiley, 1979.

[22] V. Y. Pan, *Structured Matrices and Polynomials: Unified Superfast Algorithms*. Birkhäuser, 2001.

[23] R. M. Gray *et al.*, *Toeplitz and circulant matrices: A review*. Now Publishers, 2006.

[24] I. J. Good, "Skew circulants and the theory of numbers," *The Fibonacci Quarterly*, vol. 24, no. 1, pp. 47–60, 1986.

[25] M. Püschel and J. M. Moura, "Algebraic signal processing theory," *arXiv preprint cs/0612077*, 2006.

[26] J. M. Lee, *Introduction to Topological Manifolds*. Springer, 2011.

[27] A. C. Antoulas, Ed., *Mathematical System Theory: The Influence of R. E. Kalman*. Springer, 1991.

[28] F. Colonius and W. Kliemann, *Dynamical Systems and Linear Algebra*. American Mathematical Society, 2014.

[29] G. Surges, T. Smyth, and M. Puckette, "Generative audio systems using power-preserving all-pass filters," *Computer Music Journal*, vol. 40, no. 1, pp. 54–69, 2016. [Online]. Available: http://www.jstor.org/stable/43830402

[30] D. Fu, Z. Jiang, Y. Cui, and S. T. Jhang, "New fast algorithm for optimal design of block digital filters by skew-cyclic convolution," *IET Signal Processing*, vol. 8, no. 6, pp. 633–638, 2014.

[31] M. C. Yesilli, S. Tymochko, F. A. Khasawneh, and E. Munch, "Chatter diagnosis in milling using supervised learning and topological features vector," in *2019 18th IEEE international conference on machine learning and applications (ICMLA)*. IEEE, 2019, pp. 1211–1218.

[32] A. Feuer and G. Goodwin, *Sampling in digital signal processing and control*. Springer, 2012.

[33] H. Osborn, *Vector Bundles, Volume 1: Foundations and Stiejel–Whitney Classes*. Academic Press, 1983.

[34] N. H. Fletcher and T. D. Rossing, *The Physics of Musical Instruments*. Springer, 1998.

[35] G. Essl, "Iterative Phase Functions on the Circle and Their Projections: Connecting Circle Maps, Waveshaping, and Phase Modulation," in *Perception, Representations, Image, Sound, Music*, R. Kronland-Martinet, S. Ystad, and M. Aramaki, Eds. Springer, 2021, pp. 681–698.

[36] R. Aldrovandi and R. da Rocha Jr, *A gentle introduction to knots, links and braids*. World Scientific, 2021.

[37] E. W. Chambers, C. Fillmore, E. Stephenson, and M. Wintraecken, "Braiding vineyards," in *Proceedings of the 2026 Annual ACM-SIAM Symposium on Discrete Algorithms (SODA)*, 2026, pp. 6240–6263.

[38] S. Kasich, "Possible applications of knots in computer music and nimes," in *Proceedings of the International Conference on New Interfaces for Musical Expression*, 2024, pp. 198–205.

[39] G. Dal Santo, K. Prawda, S. J. Schlecht, and V. Välimäki, "Optimizing tiny colorless feedback delay networks," *EURASIP Journal on Audio, Speech, and Music Processing*, vol. 2025, no. 1, p. 13, 2025.